

Period-doubling bifurcations in detuned lasers with injected signals

Kenju Otsuka and Hitoshi Kawaguchi

Musashino Electrical Communication Laboratory, Nippon Telegraph and Telephone Public Corporation, Musashino-shi, Tokyo 180, Japan

(Received 19 December 1983)

Detuned-lasers systems which have anomalous dispersion effects at the lasing wavelength are predicted to have period-doubling bifurcations for injected light signals. The basic idea is derived from the dependence of the active-region refractive index on population inversion density. The response of detuned lasers with injected light signals is shown to be governed by the generalized Van der Pol equations with external driving forces that are nonlinear in nature. Experimental results with a LiNdP₄O₁₂ miniature solid-state laser are shown, demonstrating period-doubling bifurcations.

Period-doubling bifurcations have been predicted for resonant-type multistable laser diode amplifiers operating in external cavities.¹ This basic idea was derived from the dependence of the active layer refractive index on carrier density. Such Ikeda-like instabilities² are to be expected in other laser amplifier systems where these are asymmetrical derivatives with respect to the population density at the lasing frequency^{1,3} or where the lasing wavelength is detuned from the gain spectrum peak (such a situation will hereafter be called a detuned-laser system).

The present Rapid Communication predicts a new class of period-doubling bifurcations and chaotic self-pulsations in detuned-laser systems having injected signals, and shows a brief experimental result as well. Optical bistability and self-pulsations with bifurcations will be shown to take place at the edge of the injection lock-in region for the low pump as well as low light injection regime due to the anomalous dispersion effect at lasing frequency.

Figure 1(a) conceptually illustrates the injection locking model used in the following analysis. It is assumed that the effects of standing-wave modulation of the population-

inversion (spatial hole burning) and propagation effect are negligible, and that mean-field approximation is employed. A coherent beam of frequency ω_i is injected into the axial mode of a laser whose frequency is $\omega_0(N)$ (N is the population-inversion density).

Taking into account the anomalous dispersion effect in a detuned-laser medium, the injection locking equations for the rotating wave approximation fields and external phase angle can be derived from the balance of the electric fields at an oscillator mirror as follows:

$$\frac{dN}{dt} = P - \frac{N}{\tau} - G(N)S, \tag{1}$$

$$\frac{dE}{dt} = \left(G(N) - \frac{1}{\tau_p} \right) \frac{E}{2} + \frac{\omega_0}{2Q} E_i \cos \psi, \tag{2}$$

$$\frac{d\psi}{dt} = \omega_0(N) - \omega_i - \frac{\omega_0}{2Q} \frac{E_i}{E} \sin \psi, \tag{3}$$

$$S \equiv E^2.$$

Here, P is the pump rate, N is the population-inversion density, S is the photon density, E is the electric field amplitude, τ is the upper-state lifetime, τ_p is the photon lifetime, G is the gain function, Q is the external quality factor of the resonator, and ψ is the external phase angle.

The dependences of G and ω_0 on N come from the fact that the active-region refractive index varies with the population-inversion density as a result of anomalous dispersion effect in the detuned-laser medium. For brevity, $G(N)$ and $\omega_0(N)$ are approximated using Taylor's series up to the first order:

$$\begin{aligned} G(N) &= G(N_{th}) + \frac{\partial G}{\partial N} (N - N_{th}) \\ &= \frac{1}{N_{th} \tau_p} + \frac{\partial G}{\partial N} (N - N_{th}), \end{aligned} \tag{4}$$

$$\begin{aligned} \omega_0(N, \Omega) &= \omega_0(N_{th}) + \frac{\partial \omega_0}{\partial N} (N - N_{th}) \\ &\quad - \left[\frac{n_e}{n} - 1 \right] [\Omega - \omega_0(N_{th})], \end{aligned} \tag{5}$$

where N_{th} is the threshold population density, Ω is the oscillation frequency, and $n_e = n + \Omega (\partial n / \partial \Omega)$ is the effective refractive index.

Here we introduce the parameter $R = -2(\partial \omega / \partial N) /$

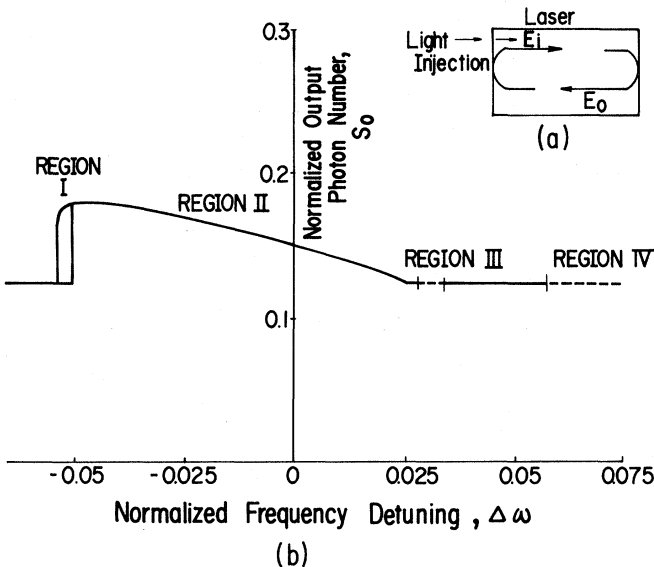


FIG. 1. (a) Conceptual model of a detuned laser with external light signals. (b) Injection-locking curve. $\omega = 1.125$, $S_i = 10^{-4}$, $R = -2$.

$(\partial G/\partial N)$, which is the ratio of the derivatives of the real part to the imaginary part of the dielectric constant with respect to population-inversion density. This defined parameter comes from the anomalous dispersion at the lasing wavelength in such a detuned-laser medium as semiconductor lasers. With semiconductor laser diodes, for example, R is reported to take on a value between -0.5 and -6.2 .⁴⁻⁶

Figure 1(b) shows the injection locking curve for which the following dimensionless parameters are introduced: $w = P/P_{th}$ (P_{th} : threshold pump rate): normalized pump rate; $S_0 = E^2/\tau_p P_{th}$: normalized photon density; $S_i = (\omega_0 E_i/2Q)^2 \tau_p/P_{th}$: normalized injected photon density; $\Delta\omega = (n_e/n)[\omega_i - \omega_0(N_{th})]\tau_p$: normalized frequency detuning. Calculations were carried out assuming $w = 1.125$, $S_i = 10^{-4}$, and $R = -2$.

The asymmetric nature of the tuning curve is apparent from this figure, and detuning characteristics were found to be dividable into the following regions: (I) a bistable region with hysteresis; (II) a stable lock-in region without bistability and instability; (III) a dynamically unstable region having pulsation solutions; (IV) a self-modulating region outside the lock-in range.

Figure 2 shows the steady-state stability diagram for injection locking as a function of the relative pump rate w , assuming $R = -2$ and $S_i = 10^{-4}$. For a low pump rate

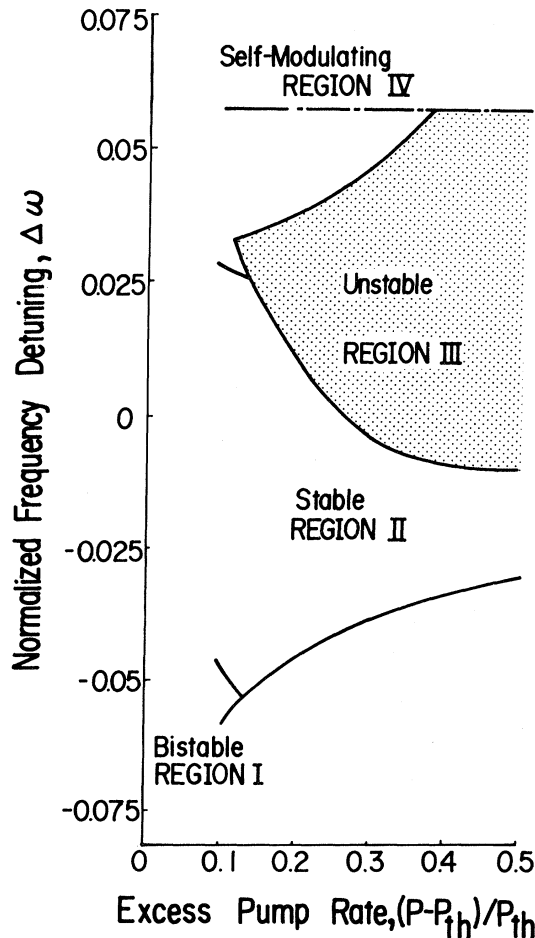


FIG. 2. Stability diagram of an injection locking in detuned lasers. $S_i = 10^{-4}$, $R = -2$.

$w \leq 1.13$, a bistable region I exists. With an increase in the pump rate, the stable lock-in region II becomes narrower and the bistable region I disappears, where the dynamic unstable region III appears instead. For $w \geq 1.4$, subharmonic bifurcations begin to take place in region III. For $w < 1.4$, however, the system shows only self-sustained pulsations, and bifurcations were found to be absent. The asymmetrical tuning curve, as well as the hysteresis properties, results from the nonlinear change in the resonant frequency coming from the dependence of the refractive index on population-inversion density, and these have been experimentally reported for semiconductor lasers.⁷⁻⁹ Self-sustained pulsations were also predicted in semiconductor lasers with injected signals.⁷

Figure 3 shows the output response for various detunings to a stepwise increase of the pump rate from $w = 1.01$ to 1.5 at $T = t/\tau_p = 200$ in regions II-IV. The adopted parameter values are $R = -2$ and $S_i = 10^{-4}$. In the stable lock-in region II, the output approaches a steady-state value with a positive damping constant [see Fig. 3(a)]. Within the dynamically unstable region III, period-doubling bifurcations of self-pulsations occur with increasing the detuning $\Delta\omega$ until chaotic self-pulsations are finally brought about [see Figs. 3(b)-3(e)]. In the self-modulating region IV, pulsations at

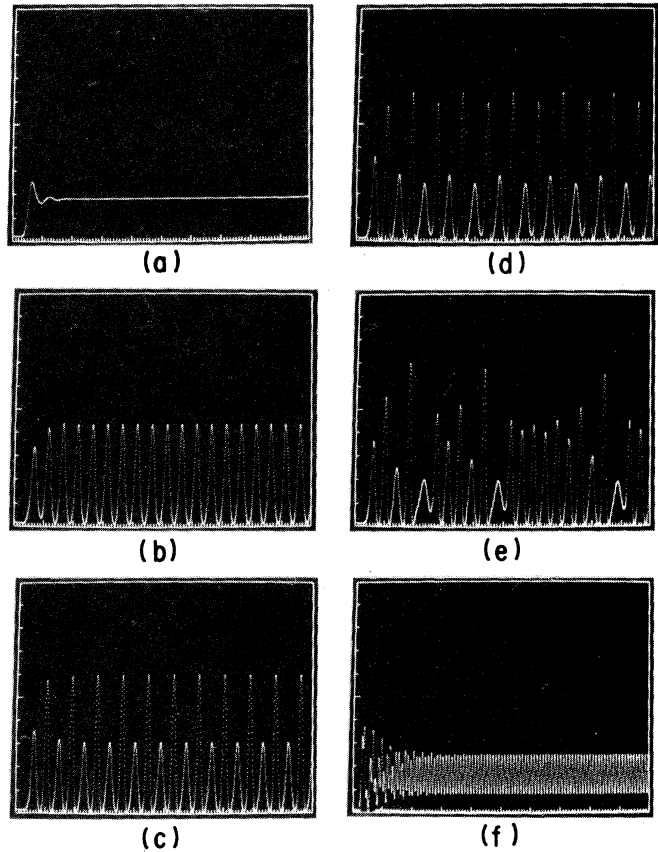


FIG. 3. Output response in the stable lock-in region II [(a)], unstable locking region III [(b)-(e)], and self-modulating region IV [(f)]. $w = 1.5$, $S_i = 10^{-4}$, $R = -2$, $\tau/\tau_p = 10^3$. Vertical axis S_0 : $0.3/\text{div}$. Horizontal axis $T = t/\tau_p$: (a)-(e) $50/\text{div}$; (f) $100/\text{div}$. (a) detuning $\Delta\omega = -0.025$, (b) 0 (period 1), (c) 0.0125 (period 2), (d) 0.0156 (period 4), (e) 0.0188 (chaotic), (f) 0.0625. Simulations were carried out based on the Runge-Kutta-Gill method.

a frequency of $\Delta\omega$ appear [see Fig. 3(f)]. This self-modulating phenomenon has already been reported to occur both theoretically^{10,11} and experimentally^{12,13} for lasers even when $R=0$. However, a dynamically unstable region III appears only when $R \neq 0$.

Self-pulsations with bifurcations can be explained in terms of the nonlinear interaction between two field components having frequencies of ω_i and $\omega_0(N)$. The nonlinear interaction of both waves produces population pulsation through the intensity beat between two waves that is nonlinear in nature. This population pulsation acts as a driving force for the laser, which is governed by the generalized Van der Pol equations (1)–(3). Temporal variations in the refractive index which are associated with such population pulsation cause asymmetrical stimulated scattering of amplified injected signals into the mode with cavity resonance frequency and give additional gain to the cavity mode at the lower frequency side when $R < 0$. This type of asymmetrical mode interaction was first observed in semiconductor lasers.¹⁴ At this point, stable injection locking breaks down, forcing the simultaneous oscillation at the resonant cavity mode. Furthermore, complex wave forms leading to chaos should be expected since the intensity beat frequency itself is a function of N .

Experiments were carried out by using a detuned-laser medium $\text{LiNdP}_4\text{O}_{12}$ (LNP) (Ref. 15) to demonstrate light-injection-induced bifurcations. Figure 4(a) shows the experimental setup. The LNP crystal was 300 μm thick and the laser resonator consisted of a flat mirror M_1 transmission at 1.32 μm ($T_1=0.1\%$) and a curved mirror M_2 ($T_2=0.5\%$, radius of curvature: 1 cm) separated by 1 cm (semiconcentric configuration). An argon laser ($\lambda=5145 \text{ \AA}$) served as a pump. The oscillation threshold was 20 mW and the slope efficiency was 10%. A cw single-axial-mode oscillation whose wavelength was detuned from the gain spectral peak was obtained. This condition was easily obtained by changing the crystal thickness slightly since the etalon effect of the LNP crystal yields the free spectral range of 18.1 \AA while the fluorescence spectral width is as small as 40 \AA .¹⁵ The light beam of the TEM_{00} mode of the LNP laser ($\lambda=1.32 \mu\text{m}$) was split into two beams and 95% of the total light was impinged on the rotating hard paper sheet with a rough surface. A monitor beam was detected with a Ge photodiode followed by a spectrum analyzer.

In this configuration, the Doppler-shifted scattered field component whose angular frequency is shifted by ω_d from ω_0 [$\omega_d = v \cos(\theta_s/\lambda)$; v : rotation velocity; θ_s : angle between the laser axis and velocity vector] acts as a delayed external injection signal E_i for the LNP laser.¹⁶ By changing the detuning, i.e., ω_d , we have measured the response of the laser. Figures 4(b) and 4(c) show measured frequency spectra for different ω_d values where $w = P/P_{\text{th}} = 4.5$. These figures clearly show the period-doubling bifurcations

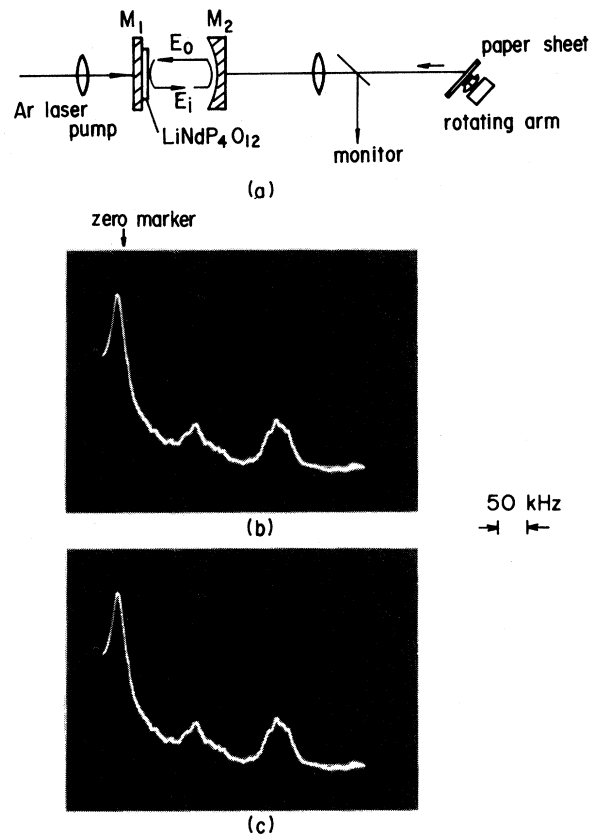


FIG. 4. (a) Experimental arrangement for demonstrating the period-doubling bifurcations. (b) Period 2 ($\omega_d/2\pi=160 \text{ kHz}$). (c) Period 4 ($\omega_d/2\pi=200 \text{ kHz}$).

[Fig. 4(b): period 2; Fig. 4(c): period 4]. We also observed the self-modulating pulsations whose repetition frequencies coincided with ω_d (region IV) at higher ω_d values.¹⁶ The observed period-doubling bifurcations may be interpreted by introducing the delayed feedback term into Eqs. (1)–(3). In the case of multiaxial-mode operations for thicker LNP crystals, such period-doubling bifurcations were not observed.¹⁶

In summary, period-doubling bifurcations of self-pulsations in detuned lasers employing injected signals, based on the anomalous dispersion effect at the lasing wavelength, have been predicted. The experimental results on period-doubling bifurcations in Nd stoichiometric lasers with Doppler-shifted delayed injection signals have been shown.

Discussions with Dr. H. Okamoto are acknowledged.

¹K. Otsuka and H. Iwamura, Phys. Rev. A **28**, 3153 (1983).

²K. Ikeda, H. Daido, and O. Akimoto, Phys. Rev. Lett. **45**, 709 (1980).

³K. Vahala, L. C. Chiu, S. Margalit, and A. Yariv, Appl. Phys. Lett. **42**, 631 (1983).

⁴D. D. Cook and F. R. Nash, J. Appl. Phys. **46**, 1660 (1975).

⁵P. A. Kirkby, IEEE J. Quantum Electron. **QE-13**, 705 (1977).

⁶C. H. Henry, R. A. Logan, and K. A. Bertness, J. Appl. Phys. **52**, 4457 (1982).

⁷R. Lang, IEEE J. Quantum Electron. **QE-18**, 976 (1982).

⁸K. Kobayashi, H. Nishimoto, and R. Lang, Electron. Lett. **18**, 54 (1982).

⁹S. Kobayashi and T. Kimura, IEEE J. Quantum Electron. **QE-17**, 681 (1981).

- ¹⁰M. B. Spencer and W. E. Lamb, Phys. Rev. A 5, 884 (1972).
- ¹¹K. Otsuka and S. Tarucha, IEEE J. Quantum Electron. QE-17, 1515 (1981).
- ¹²J.-I. Nishizawa and K. Ishida, IEEE J. Quantum Electron. QE-11, 515 (1975).
- ¹³V. Annovazzi Lodi and S. Donai, IEEE J. Quantum Electron. QE-16, 859 (1980).
- ¹⁴A. P. Bogatov, P. G. Eliseev, and B. N. Sverdlov, IEEE J. Quantum Electron. QE-11, 510 (1975).
- ¹⁵M. Saruwatari, K. Otsuka, S. Miyazawa, and T. Kimura, IEEE J. Quantum Electron. QE-13, 836 (1977).
- ¹⁶K. Otsuka, IEEE J. Quantum Electron. QE-15, 655 (1979).

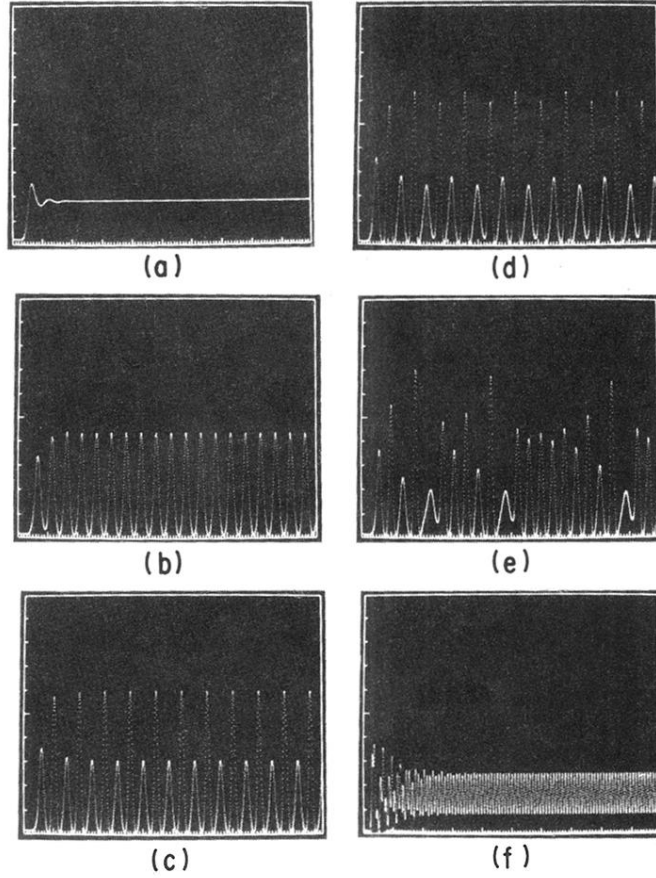


FIG. 3. Output response in the stable lock-in region II [(a)], unstable locking region III [(b)–(e)], and self-modulating region IV [(f)]. $w=1.5$, $S_i=10^{-4}$, $R=-2$, $\tau/\tau_p=10^3$. Vertical axis S_0 : 0.3/div. Horizontal axis $T=t/\tau_p$: (a)–(e) 50/div.; (f) 100/div. (a) detuning $\Delta\omega=-0.025$, (b) 0 (period 1), (c) 0.0125 (period 2), (d) 0.0156 (period 4), (e) 0.0188 (chaotic), (f) 0.0625. Simulations were carried out based on the Runge-Kutta-Gill method.